Inorg. Chem. **2008**, *47*, 6137−6143

Inorganic Chemistry Article

Can Undoped Calcium Tetraborides Exist? An Answer from the Comparison of Its Density Functional Theory Electronic Structure with that of Rare-Earth Metal Tetraboride

Mouna Ben Yahia,[†] Olaf Reckeweg,[‡] Régis Gautier,[†] Joseph Bauer,[†] Thomas Schleid,[‡] Jean-François Halet,[*,†] and Jean-Yves Saillard[*,†]

Sciences Chimiques de Rennes, UMR 6226 CNRS − ENSC Rennes - Université de Rennes 1, Avenue du Général Leclerc, F-35042 Rennes Cedex, France, and Institut für Anorganische Chemie der Universität Stuttgart, Pfaffenwaldring 55, D-70569 Stuttgart, Germany

Received October 5, 2007

Periodic density functional theory calculations are used to discuss the existence of metal tetraborides MB_4 with divalent metals. Tetraborides which contain metal atoms inserted in a three-dimensional boron network made of B_6 octahedra and B_2 dumbbells exhibit a pseudo energy gap for a count of 60 valence electrons per $M_4(B_6)_2(B_2)_2$ formula unit. Such a count satisfies the stability electron requirement for B_6^{2-} (20 electrons) octahedra and B_2^{2-} (8 electrons) units and allows the filling of two supplementary low-lying bands deriving from the valence metallic d atomic orbitals. This favored electron count is not reached for CaB_4 which is then formally deficient by one electron per metal atom. This indicates that CaB_4 is unlikely to exist without *n*-doping.

Introduction

Borides of Group 1, 2, and 3 metals are known for exhibiting extended 2-dimensional (2D) or 3-dimensional (3D) networks of boron.[1] Typical examples are superconducting MgB_2 in which the boron atoms are arranged in graphite-like layers[2] and CaB_6 in which boron octahedra are linked to each other through intercluster B−B bonds in the three directions, forming a simple cubic packing.[3] It is often possible to rationalize the structural arrangement of these compounds in terms of simple electron counting rules within the ionic “Zintl−Klemm” bonding scheme, that is, assuming a fully oxidized metal cation sublattice interacting with an anionic boron network. For example, in MgB_2 [$Mg^{2+}(B^-)_2$] the B^- atoms satisfy the octet rule in the same manner as C does in graphite. Similarly, in CaB_6 [$Ca^{2+}(B_6)^{2-}$] the $(B_6)^{2-}$ octahedra satisfy the electron counting rules of the polyhedral-skeletal-electron-pair (PSEP) theory,[4] with 7 skeletal electron pairs for intracluster bonding and 6 electrons (one on each boron atom) for making 6 intercluster localized 2-electron/2-center bonds.[5] Because both Ca^{2+} and $(B_6)^{2-}$ satisfy the closed-shell requirement, CaB_6 is a semiconductor at ambient pressure.[6] However, deviations away from these electron-counting rules can occur. For example, the conducting compounds KB_6[7] and LaB_6,[8] which are isostructural to CaB_6, are lacking and exceeding one electron per B_6 unit, respectively, for satisfying the PSEP rules. In the former case, the

* To whom correspondence should be addressed. E-mail: halet@univ-rennes1.fr (J.-F.H.), saillard@univ-rennes1.fr (J.-Y.S.).

† Université de Rennes 1.

‡ Institut für Anorganische Chemie der Universität Stuttgart.

(1) Etourneau, J. In *Inorganic Reactions and Methods*; Zuckerman, J. J., Hagen, A. P., Eds; VCH: New York, 1991; Vol. *13*, pp 167−196.

(2) (a) Nagamutsu, J.; Nakagawa, N.; Muranaka, T.; Zenitani, Y.; Akimitsu, J. *Nature* **2001**, *2*, 43. (b) Buzea, C.; Yamashita, T. *Supercond. Sci. Technol.* **2001**, *14*, R115.

(3) (a) von Stackelberg, M.; Neumann, F. *Z. Phys. Chem.* **1932**, *B19*, 314. (b) Naslain, R.; Etourneau, J. *C. R. Acad. Sci.* **1966**, *263*, 484. (c) Etourneau, J.; Naslin, R.; Laplaca, S. *J. Less-Common Met.* **1971**, *24*, 183.

(4) See for example (a) Wade, K. *Chem. Commun.* **1971**, *15*, 792. (b) Mingos, D. M. P. *Nature (London) Phys. Sci.* **1972**, *236*, 99. (c) Wade, K. *Adv. Inorg. Chem. Radiochem.* **1976**, *18*, 1. (d) Mingos, D. M. P. *Acc. Chem. Res.* **1984**, *17*, 311. (e) Mingos, D. M. P. ; Wales, D. J., *Introduction to Cluster Chemistry*; Prentice-Hall: Englewood Cliffs, NJ, 1990.

(5) (a) Denlinger, J. D.; Clack, J. A.; Allen, J. W.; Gweon, G.-H.; Poirier, D. M.; Olson, C. G.; Sarrao, J. L.; Bianchi, A. D.; Fisk, Z. *Phys. Rev. Lett.* **2002**, *89*, 157691. (b) Cho, B. K.; Rhyee, J.-S.; Oh, B. H.; Jung, M. H.; Kim, H. C.; Yoon, Y. K.; Kim, J. H.; Ekino, T. *Phys. Rev. B* **2004**, *69*, 113202.

(6) (a) Perkins, P. G. *Boron and Refractory Borides*; Maktovich, V. I., Ed.; Spinger-Verlag: Berlin, 1977; pp 31−51. (b) Tromp, H. J.; van Gelderen, P.; Kelly, P. J.; Brocks, G.; Bobberts, P. A. *Phys. Rev. Lett.* **2001**, *87*, 16401. (c) Hiono, H.; Aryasetiawan, F.; von Schilfgaarde, M.; Kotani, T.; Miyake, T.; Terakura, K. *J. Phys. Chem. Solids* **2002**, *63*, 1595. (d) Schmitt, K.; Stückl, C.; Ripplinger, H.; Albert, B. *Solid State Sci.* **2001**, *3*, 321. (e) Wu, Z.; Singh, D. J.; Cohen, R. E. *Phys. Rev. B* **2004**, *69*, 193105. (f) Lee, B.; Wang, L.-W. *Appl. Phys. Lett.* **2005**, *87*, 262509.

10.1021/ic701967n CCC: $40.75
Published on Web 06/24/2008

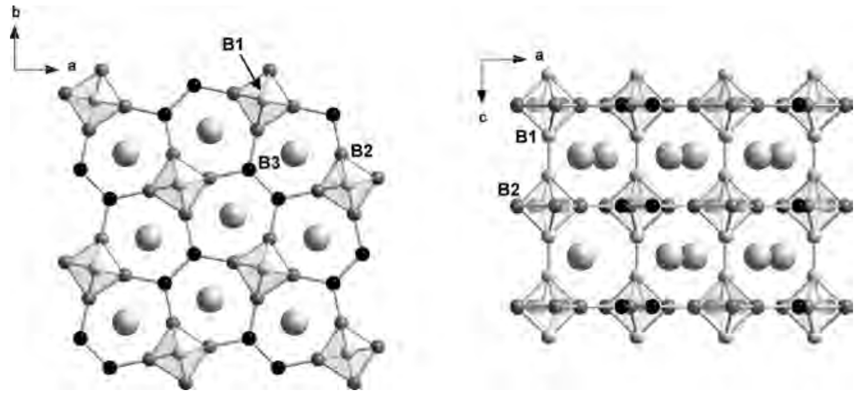

Figure 1. ThB_4-type crystal structure. Projections down (left) and along (right) the *c* axis. Large gray spheres and small black or gray spheres represent metal and boron atoms, respectively.

$(B_6)^-$ octahedra tend to compensate their electron deficiency by forming bipolarons, that is, weak Jahn−Teller coupling between neighboring octahedra.[7] It has been claimed that KB_6 is stabilized by carbon insertion.[8] Interestingly, NaB_6 seems to be stable only when it is doped with a substantial amount of carbon to reach the NaB_5C composition.[8] In LaB_6, the excess electron is shared between the B_6 units and La, thus leading to a metal formal charge intermediate between +2 and +3.[9]

Metal Tetraborides. Electron Counting Considerations. Tetragonal (*P*4/*mbm*) rare-earth metal tetraborides of the ThB_4[10,11] structure-type have a somewhat more complicated architecture. They also contain B_6 octahedra, but in that case they are directly bonded to each other only in the *c* direction. In the *ab* plane, the B_6 octahedra are linked to each other through B_2 units (see Figure 1). These units are made of sp^2-hybridized boron atoms (labeled B3 in Figure 1), each of them being bonded to two B_6 octahedra and to its partner in the B3−B3 unit. The three corresponding bond lengths are of the same order of magnitude (∼1.7−1.8 Å). Therefore, MB_4 (M = rare-earth metal) can be reformulated $M_2(B_6)(B_2)$. The question which arises then is the formal charge distribution between *M*, the B_6, and the B_2 units. While a charge of 2− can easily be attributed to the B_6 octahedron by analogy with CaB_6, the charge attribution for the B_2 units is not so straightforward. Assuming localized 2-electron/2-center bonding around these atoms leads to three possible electron counts, each corresponding to one of the Lewis formulas given in Scheme 1. The bonding scheme depicted in Scheme 1*a* is satisfactory from the point of view of boron bonding because it corresponds to planar tricoordinated atoms obeying the sextet rule, a situation not uncommon in boron molecular chemistry.[12] However, it is less satisfactory from the point of view of the formal charge balance, that is, $(M^+)_2(B_6^{2-})(B_2)$ because it leaves a generally trivalent metal in an unrealistically low oxidation state. The situation in Scheme 1*b* exhibits negatively charged sp^2-hybridized boron atoms which satisfy the octet rule. The charge partitioning $(M^{2+})_2(B_6^{2-})(B_2^{2-})$ is more realistic for *M*, but the B3−B3 interatomic distance does not show a strong tendency for multiple bonding in any of the structurally characterized compounds of this type.[10,11] The charge partitioning associated with Scheme 1*c*, $(M^{3+})_2(B_6^{2-})(B_2^{4-})$, corresponds to a fully oxidized metal, a B3−B3 single bond, and B3 atoms satisfying the octet rule. However, in such a situation the sp^2 hybridization of boron should be disfavored over the nonplanar sp^3 one. Moreover, the coexistence in the same structure of particularly electron-rich B^{2-} atoms, bearing a nonbonding lone-pair, with electron-poor B_6^{2-} clusters does not look *a priori* reasonable. Thus, none of the charge partitioning is at first sight fully satisfactory. Previous tight-binding calculations on GdB_4 carried out in our group at the extended Hückel level concluded that the Lewis formula (Scheme 1*b*) is the one which provides the best description of the bonding in this compound.[11] It was suggested that the formal B3=B3 double bond was particularly weak because of its coordination to the Gd atoms.

Scheme 1

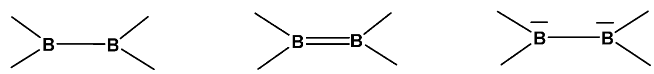

$(B_2)^0$ (*a*) $(B_2)^{2-}$ (*b*) $(B_2)^{4-}$ (*c*)

From these results, it appears reasonable to describe GdB_4 (or any rare-earth metal tetraboride) as an electron-rich compound with respect to a hypothetical semiconducting

(7) (a) Etourneau, J.; Ammar, A.; Villesuzanne, A.; Villeneuve, G.; Chevalier, B.; Whangbo, M.-H. *Inorg. Chem.* **2003**, *42*, 4242. (b) Ammar, A.; Ménétrier, M.; Villesuzanne, A.; Matar, B.; Chevalier, B.; Etourneau, J.; Villeneuve, G.; Rodriguez- Carvajal, J.; Koo, H. J.; Smirnov, A. I.; Whangbo, M.-H. *Inorg. Chem.* **2004**, *43*, 4974.
(8) Albert, B.; Schmitt, K. *Chem. Mater.* **1999**, *11*, 3406.
(9) (a) Korsukova, M. M.; Gurin, V. N.; Lundström, T.; Tergenius, L.-E. *J. Less-Common Met.* **1986**, *117*, 73. (b) Kimura, S.; Nanba, T.; Tomikawa, M.; Kunii, S.; Kasuya, T. *Phys. Rev. B* **1992**, *46*, 12196. (c) Hossain, F. M.; Riley, D. P.; Murch, G. E. *Phys. Rev. B* **2005**, *72*, 235101.
(10) (a) Zalkin, A.; Templeton, D. H. *Acta Crystallogr.* **1953**, *6*, 269. (b) Giese, R. F., Jr.; Matkovich, V. I.; Economy, J. *Z. Kristallogr.* **1965**, *122*, 423. (c) Schäfer, W.; Will, G. *Z. Kristallogr.* **1976**, *144*, 217. (d) Guette, A.; Vlasse, M.; Etourneau, J.; Naslain, R. *C. R. Acad. Sci. C* **1980**, *291*, 145. (e) Will, G.; Schäfer, W.; Pfeiffer, F.; Elf, F. *J. Less-Common Met.* **1981**, *82*, 349. (f) Zavalii, L. V.; Bruskov, V. A.; Kuz'ma; Yu., B. *Inorg. Mater.* **1988**, *24*, 1350. (g) Salamakha, P.; Gonçalves, A. P.; Sologub, O.; Almeida, M. *J. Alloys Compd.* **2001**, *316*, L4.
(11) Garland, M. T.; Wiff, J. P.; Bauer, J.; Guérin, R.; Saillard, J.-Y. *Solid State Sci.* **2003**, *5*, 705.
(12) Albright, T. A.; Burdett, J. K.; Whangbo, M.-H. *Orbital Interactions in Chemistry*; Wiley: New York, 1985.

CaB_4 compound, in the same way as LaB_6 is electron-rich relatively to the well-known semiconducting CaB_6 compound. It turns out that recently Meyer et al. published the synthesis and characterization of a carbon-doped calcium tetraboride ($CaB_{4-x}C_x$) in which the carbon content x is lower than 5%.[13] According to these authors, "upon first glance, it could be assumed that carbon may have a stabilizing effect... This simple consideration does not, however, satisfy the distinct bonding requirements with cations...". In other words, it has not been possible to synthesize pure CaB_4 so far. However, the extended Hückel tight-binding calculations carried out by the same authors on pure CaB_4 show a small but clear band gap at the Fermi level, confirming the stable closed-shell configuration associated with the $(Ca^{2+})_2(B_6^{2-})(B_2^{2-})$ formal charge partitioning.[13]

Density functional theory (DFT) calculations were carried out on YB_4, GdB_4, and hypothetical CaB_4 to first check the validity of our previous tight-binding study on GdB_4[11] and then investigate the stability of hypothetical CaB_4. The main results are reported here.

Computational Details

Self-consistent *ab initio* band structure calculations of MB_4 were performed with the scalar relativistic tight-binding linear muffin-tin orbital method in the atomic spheres approximation including the combined correction (LMTO).[14] Exchange and correlation were treated in the local density approximation using the von Barth−Hedin local exchange correlation potential.[15] Within the LMTO formalism, interatomic spaces are filled with interstitial spheres. Because of the closed packed character of the MB_4 crystallographic structure, no interstitial "empty" spheres were added. The full LMTO basis set consisted of 6s, 6p, 5d, and 4f functions for Gd spheres, 5s, 5p, 4d, and 4f functions for Y spheres, 4s, 4p, and 3d functions for Ca spheres, and 2s, 2p, and 3d functions for B spheres. Unless specified, the eigenvalue problem was solved using the following minimal basis set obtained from Löwdin downfolding technique: Gd (6s, 5d, 4f), Y (5s, 4d), Ca (4s, 3d), and B (2s, 2p). The k space integration was performed using the tetrahedron method.[16] Charge self-consistency and the average properties for GdB_4, YB_4, and CaB_4 were obtained from 96 irreducible k points. The density of states (DOS) and crystal orbital Hamiltonian population (COHP)[17] curves were shifted so that the Fermi level lies at 0 eV. The electron localization function (ELF) was evaluated according to ref 18 within the TB-LMTO-ASA program package. To get more insight into the chemical bonding, ELF was analyzed with the program Basin.[19] An integration of the valence electron density in the basins defined by surfaces of zero flux in ELF gradient gave, analogously to the procedure proposed by Bader for the electron density,[20] the electron counts for each basin, which are important for the description of the bonding situation.

Full optimizations of the atomic positions and cell parameters were carried out on MB_4 using the Vienna Ab initio Simulation package (VASP).[21] Ion cores were represented by projector augmented wave (PAW) pseudopotentials provided within the program.[22] The Perdew−Burke−Ernzerhof (PBE) generalized gradient approximation (GGA) was employed for the exchange and correlation energy term.[23] The Brillouin zone was sampled using a $8 \times 8 \times 16$ Monkhorst−Pack grid. A plane wave basis set with a cutoff energy of 600 eV was used to construct the valence electronic wave functions.

Phonon calculations were performed using the direct approch.[24] A displacement of 0.015 Å was used to move the atoms from their equilibrium position and then to calculate the Hessian matrix. The eigenvalues (frequencies) were obtained by diagonalizing the dynamical matrix.

Experimental and optimized crystallographic parameters, as well as the corresponding bond distances of MB_4 compounds (M = Y, Gd, Ca) are shown in Table 1.

Discussion

Electronic Structure of the Anionic Boron Network. We start the analysis by looking at the electronic structure of the anionic $(B_4)^{2-}$, that is, $[(B_6)(B_2)]^{4-}$ 3D sublattice of CaB_4 which was computed using the artifact of removing all the functions centered on calcium atoms leading to a total transfer of their two valence electrons to the boron network. The total DOS shows a gap of about 1.6 eV for the 2− charge. Of interest is the projected DOS of B3, the boron atoms of the B_2 dumb-bells, shown in Figure 2. The highest occupied band and the lowest vacant one are dominantly B3($2p_\pi$) in character. The B3−B3 COHP curve shows that the former is bonding and the latter antibonding. This is indicative of the existence of a B3═B3 double bond, at least in the isolated hypothetical $[(B_6)(B_2)]^{4-}$ sublattice.

Electronic Structure of the Rare-Earth Metal Tetraborides. The total and projected DOS of MB_4 are shown in Figure 3 and 4 for M = Y and Gd, respectively. For both compounds, the shape of the total DOS exhibits a deep minimum (close to zero) at the Fermi level. In other words, the pseudogap at the Fermi level corresponds to 2 more electrons per $Gd_2(B_6)(B_2)$ formula than that corresponding to formally $(B_6)^{2-}$ and $(B_2)^{2-}$ units. This may suggest $(B_2)^{4-}$ rather than $(B_2)^{2-}$ units. Otherwise, assuming $(B_2)^{2-}$ units (thus M^{2+} metals) one may have expected a more "metallic-like" DOS shape, with a significant metal contribution at the Fermi level. Although the projections on the metal are consistent with a high oxidation state, in both cases they show a significant metal

(13) Schmitt, R.; Blaschkowski, B.; Eichele, K.; Meyer, H.-J. *Inorg. Chem.* **2006**, *45*, 3067.
(14) (a) Andersen, O. K. *Phys. Rev. B* **1975**, *12*, 3060. (b) Andersen, O. K. *Europhys. News* **1981**, *12*, 4. (c) Andersen, O. K. In *The Electronic Structure Of Complex Systems*; Phariseau, P., Temmerman, W. M., Eds.; Plenum: New York, 1984. (d) Andersen, O. K.; Jepsen, O. *Phys. Rev. Lett.* **1984**, *53*, 2571. (e) Andersen, O. K.; Jepsen, O.; Sob, M. *Electronic Band Structure and Its Application*; Yussouf, M., Ed.; Springer-Verlag: Berlin, 1986. (f) Skriver, H. L. *The LMTO Method*; Springer-Verlag: Berlin, 1984.
(15) von Barth, U.; Hedin, L. *J. Phys. C.* **1972**, *5*, 1629.
(16) Blöchl, P. E.; Andersen, O. K. *Phys. Rev. B* **1994**, *49*, 16223.
(17) Dronskowski, R.; Blöchl, P. E. *J. Phys. Chem.* **1993**, *97*, 8617.
(18) Savin, A.; Jepsen, O.; Flad, J.; Andersen, O. K.; Preuss, H.; von Schnering, H. G. *Angew. Chem., Int. Ed.* **1992**, *31*, 185.
(19) Kohout, M. *Basin*, Version 2.3. Max-Planck-Institut für Chemische Physik fester Stoffe: Dresden, Germany, 2001.
(20) Bader, R. F. W. *Atoms in Molecules: A Quantum Theory*; Oxford University Press: Oxford, 1999.
(21) (a) Kresse, G.; Hafner, J. *Phys. Rev. B* **1993**, *47*, 558. (b) Kresse, G.; Hafner, J. *Phys. Rev. B* **1994**, *49*, 14251. (c) Kresse, G.; Furthmuller, J. *Comput. Mater. Sci.* **1996**, *6*, 15. (d) Kresse, G.; Furthmuller, J. *Phys. Rev. B* **1996**, *54*, 11169.
(22) (a) Blöchl, P. E. *Phys. Rev. B* **1994**, *50*, 17953. (b) Kresse, G.; Joubert, D. *Phys. Rev. B* **1999**, *59*, 178.
(23) (a) Perdew, J. P.; Burke, K.; Ernzerhof, M. *Phys. Rev. Lett.* **1996**, *77*, 3865 Erratum, *Phys. Rev. Lett.* **1997**, *78*, 1396.
(24) Kresse, G.; Futhmüller, J.; Hafner, J. *Europhys. Lett.* **1995**, *32*, 729.

Table 1. Experimental and Computed Cell Parameters and Bond Distances in Some MB_4 Compounds [a]

	structure					
	YB_4 (exp.)[10d]	YB_4 (calc.)	GdB_4 (exp.)[11]	GdB_4 (calc.)	$CaB_{3.75}$ $C_{0.25}$ (exp.)[13]	CaB_4 (calc.)
a (Å)	7.111 (3)	7.111	7.1316 (2)	7.137	7.0989 (7)	7.158
c (Å)	4.017 (2)	4.029	4.0505 (2)	4.047	4.1353 (5)	4.095
volume (Å^3)	203.1 (2)	203.7	206.01 (1)	206.2	208.40 (4)	209.8
			Bonds (Å)			
M−M[b]	3.663 (2)	3.660	3.682 (1)	3.689	3.637	3.694
	4.000 (2)	4.029	4.051 (1)	4.047	3.682	3.766
M−B[b]	2.728 (4)	2.732	2.738 (2)	2.740	2.738 (1)	2.745
	2.850 (2)	2.858	2.873 (2)	2.876	3.142 (2)	3.090
B1−B1	1.622 (4)	1.640	1.64 (1)	1.650	1.697 (4)	1.685
B1−B2	1.747 (3)	1.752	1.759 (5)	1.756	1.773 (2)	1.758
B2−B2	1.810 (3)	1.813	1.815 (6)	1.816	1.822 (2)	1.811
B2−B3	1.721 (3)	1.720	1.729 (5)	1.728	1.729 (2)	1.749
B3−B3	1.752 (3)	1.747	1.75 (1)	1.757	1.670 (5)	1.729

[a] See Figure 1 for boron atom numbering. [b] Range.

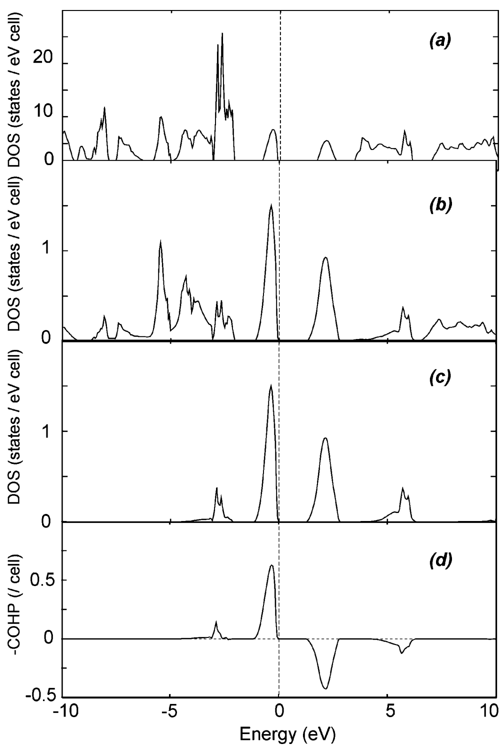

Figure 2. (a) Total DOS of the $[(B_6)(B_2)]^{4-}$ sublattice, (b) total atomic DOS of B3, (c) B3(2p$_\pi$) projected DOS, and (d) B3(2p$_\pi$)−B3(2p$_\pi$) COHP in the $[(B_6)(B_2)]^{4-}$ sub-lattice.

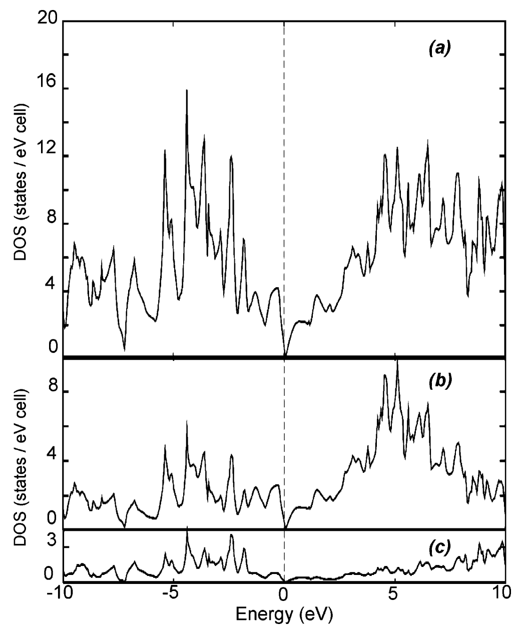

Figure 3. Total DOS and projected DOS of YB_4: (a) total, (b) Y projection, and (c) B3 contribution.

participation to the occupied states. Indeed, the metallic character is rather homogeneously dispersed over a large energy range below the Fermi level. Similar results were reported for YB_4 by Herzig and co-workers.[25]

The projected DOS of the B3(2p$_\pi$) atomic orbitals of YB_4 are shown in Figure 5a. It corresponds to an occupation slightly below 50%. The B3(2p$_\pi$)-B3(2p$_\pi$) COHP curve, which is shown in Figure 5b indicates that all the occupied B3(p$_\pi$) states are bonding, whereas most of the vacant states are antibonding. This is consistent with the existence of a π bond between the B3 atoms which is partly delocalized over the metals, *i.e.*, π donation to the metal depopulates the bonding B3(2p$_\pi$) states which mix somewhat with the empty metallic states.

The integrations of the various B−B COHP curves over the occupied states (ICOHP) are given in Table 2 for YB_4 and GdB_4. Although such values cannot be compared between different compounds, they exhibit similar trends within each compound. As expected, the values corresponding to the bonds inside the electron-deficient B_6 octahedron are significantly lower than the values corresponding to the other bonds which are localized. Among the latter, the shorter one, that is, the interoctahedra bond, appears to be the strongest. This is likely due to hyperconjugation between neighboring octahedra. It is noteworthy that the weakest of the three localized bonds is B3−B3 in both compounds. Clearly, the formally B3═B3 double bond is particularly weak, mainly because of the B3−B3 π electron donation to the metal. Thus, the Lewis formula in Scheme 1*b* should be corrected by resonant structures such as those shown in Scheme 2.

The existence of a weak double bond is also ascertained by an ELF analysis.[18] A plot of this function (η = 0.8), shown in Figure 6 for both compounds, exhibits around the

(25) Jäger, B.; Paluch, S.; Wolf, W.; Herzig, P.; Zogał, O. J.; Shitsevalova, N.; Paderno, Y. *J. Alloys Compd.* **2004**, *383*, 232.

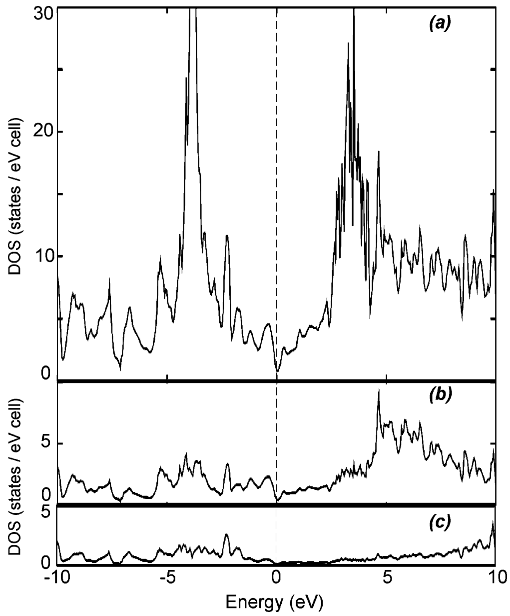

Figure 4. Total DOS and projected DOS of GdB_4: (a) total, (b) Gd projection, and (c) B3 contribution.

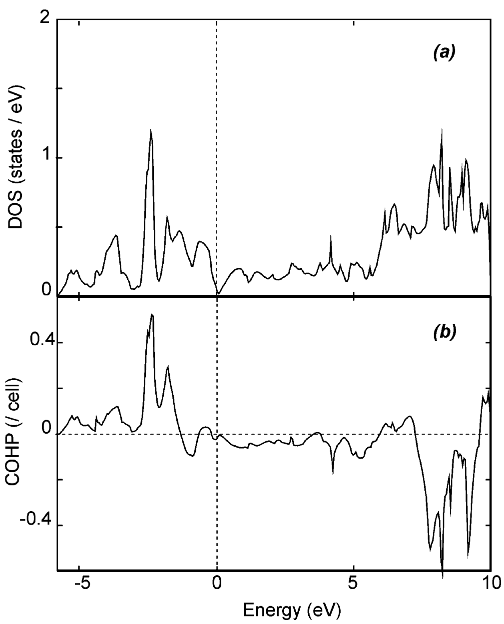

Figure 5. (a) Projected DOS of the B3(2p$_\pi$) atomic orbitals and (b) B3(2p$_\pi$)-B3(2p$_\pi$) COHP of YB_4.

Table 2. ICOHPs and Basin Charges in YB_4, GdB_4, and CaB_4 [a]

	YB_4		GdB_4		CaB_4	
bond	ICOHP	charge	ICOHP	charge	ICOHP	charge
B1−B2 B2−B2	0.6	12.3	0.6	12.0	0.6	12.0
B3−B3	0.9	3.8	0.9	3.9	1.0	3.0
B1−B1	1.1	2.4	1.2	2.4	1.1	2.3
B2−B3	1.0	2.5	1.0	2.5	1.0	2.5

[a] B−B ICOHPs are compared to B2−B3 ICOHPs which are arbitrarily set at one.

B3−B3 bond an envelope shape which resembles more that of a typical double bond rather than that of a single bond as it is around the B2−B3 and B1−B1 contacts. Basin integrated charges support this statement (Table 2). The charge computed for the whole B_6 octahedron is very close

Scheme 2

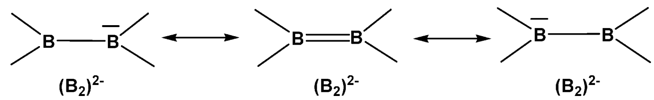

to the count of 20 electrons expected for a B_6^{2-} cluster. The charge computed for the stronger (and shorter) B1−B1 bond is smaller than that found for the B2−B3 and B3−B3 bonds. The latter value is close to 4, the ideal number for a double bond. The two former values are somewhat larger than the ideal value of 2 corresponding to a single bond, indicative of some hyperconjugation and π conjugation, respectively. Thus, all the results are consistent with the $(M^{2+})_2(B_6^{2-})(B_2^{2-})$ charge partitioning, that is, the existence of one electron per metal atom lying in a d-type band. Interestingly, however, there is an unexpected pseudogap at the Fermi level which would fit better with the $(M^{3+})_2(B_6^{2-})(B_2^{4-})$ charge partitioning.

Electronic Structure of Undoped CaB_4. What about undoped CaB_4? The total and projected DOS of CaB_4 are shown in Figure 7. Contrarily to the total DOS computed at the extended Hückel level by Meyer et al.,[13] the DFT one does not show any gap or pseudo gap at the Fermi level.

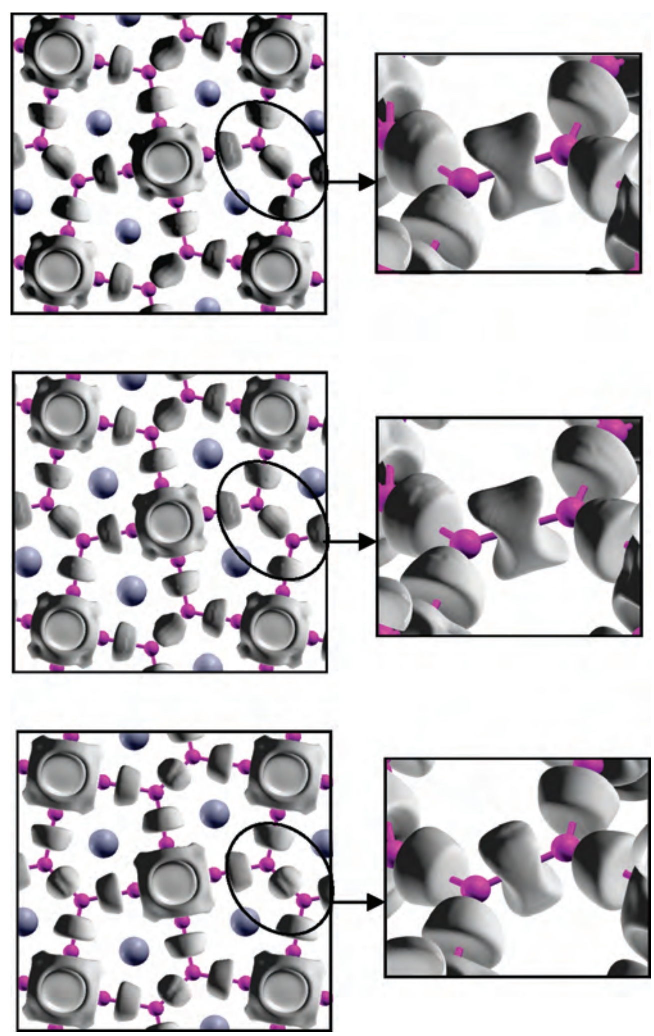

Figure 6. ELF plot of the B3−B3 bond for YB_4 (top), GdB_4 (middle), and CaB_4 (bottom).

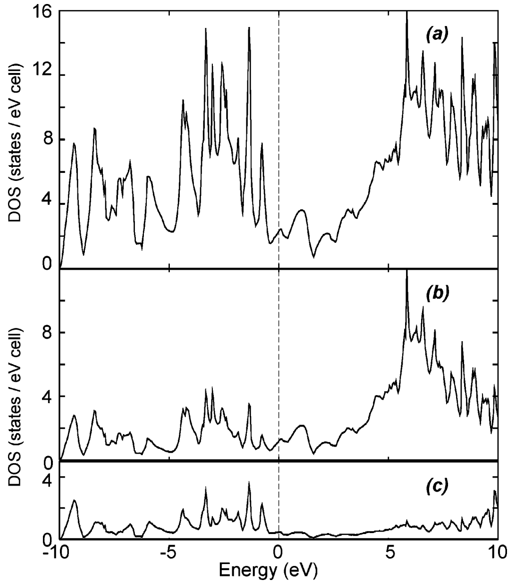

Figure 7. Total DOS and projected DOS of CaB_4: (a) total, (b) Ca projection, and (c) B3 contribution.

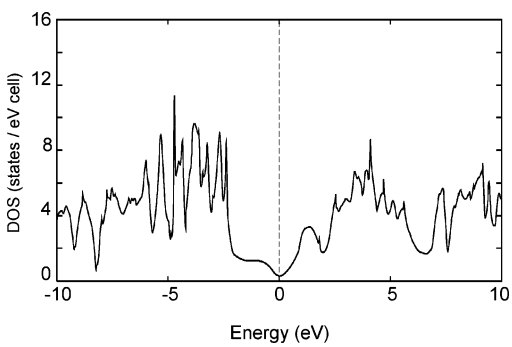

Figure 8. Total DOS of CaB_4 without Ca d states.

Rather, a pseudo gap arises for a Fermi level which would correspond to (almost) one extra electron per CaB_4 repeat unit and thus to the electron count of YB_4 or GdB_4. When the 3d atomic orbitals of Ca are not taken into account in the calculations, the pseudo gap adjusts to the Fermi level (Figure 8), quite similarly to the extended Hückel calculations of Meyer et al.[13] It turns out that in the MB_4 series (M = Y, Gd, Ca), the low lying bands below the pseudo gap are associated with occupied levels of the B_6^{2-} and B_2^{2-} units, as well as what corresponds approximately to two metallic d-bands (per M_4B_{16} formula, the content of the unit cell). These low-lying metallic bands mix strongly with the boron ones. Consequently, they are difficult to identify. Nevertheless, the bands close to the Fermi level exhibit a large metallic character, as it can be seen on the fat-band structures of YB_4 and CaB_4 shown in Figure 9. This representation shows that these two supplementary bands lie below the pseudo gap. Clearly, extended Hückel tight-binding calculations, which usually do not use d-orbitals in the basis set for Ca, are unable to reproduce the pseudogap corresponding to 15 valence electrons per MB_4 repeat unit.

The projected DOS of the B3($2p_\pi$) atomic orbitals of CaB_4 and the corresponding B3($2p_\pi$)−B3($2p_\pi$) COHP curve (Figure 10) resemble those of YB_4. Thus, the electronic structures of CaB_4 and YB_4 are related, except

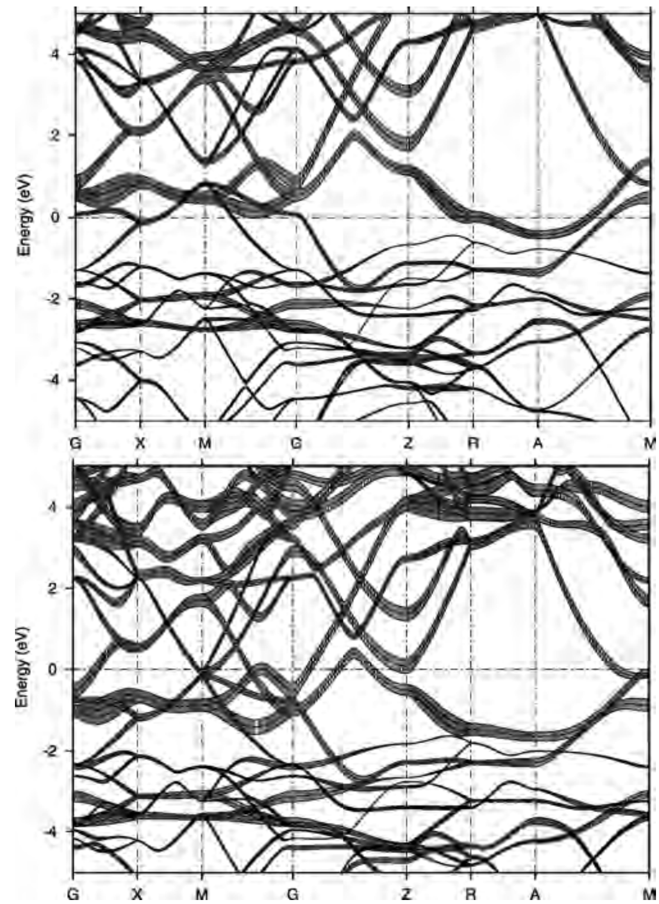

Figure 9. d-Type fat-band structures of CaB_4 (top) and YB_4 (bottom).

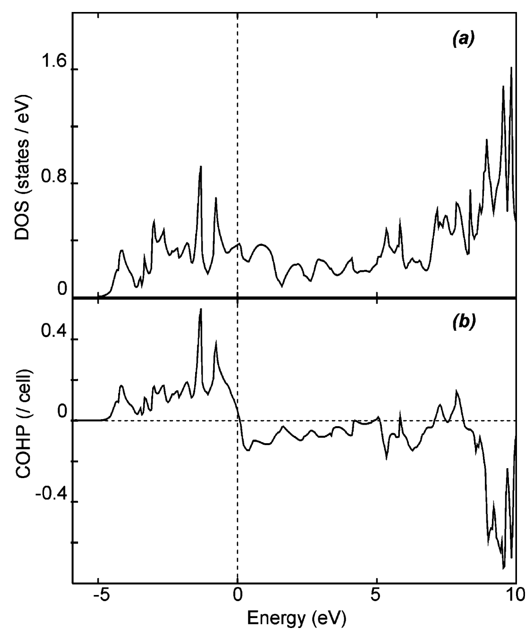

Figure 10. (a) Projected DOS of the B3($2p_\pi$) atomic orbitals and (b) B3($2p_\pi$)−B3($2p_\pi$) COHP of CaB_4.

that CaB_4 has one less electron. The shape of the ELF plot ($\eta = 0.8$) (Figure 6, bottom) is less characteristic of a double bond than that of YB_4. Basin integrated charges (Table 2) indicate a B3−B3 value lower than 4. Clearly, the electron-deficiency of CaB_4 with respect to YB_4 is shared on the metal and B3 atoms.

Phonon vibrations were computed at the Γ point in the Brillouin zone on the optimized structures of CaB_4 and YB_4. Interestingly, the results show that for the former, the calcium compound, a dozen of imaginary frequencies are obtained varying from 80i to 680i cm^{-1}, whereas for the latter, the yttrium compound, the imaginary frequencies do not exceed 3i cm^{-1}, a value much lower than the computational accuracy limit. These results support the idea that undoped CaB_4 is not stable.

Carbon Position in the Carbon-Doped Phase $CaB_{3.75}C_{0.25}$. The B3−B3 bond distance is 1.670 Å in the carbon-doped phase $CaB_{3.75}C_{0.25}$.[13] It is significantly shorter than the corresponding bond distance generally measured in other metal tetraborides which are about 1.75 Å (see Table 1). This might indicate that the C atoms occupy the B3 position. This is supported by theoretical calculations carried out on $CaB_{3.75}C_{0.25}$ ($Ca_4B_{15}C$). Indeed $Ca_4B_{15}C$ was optimized at the DFT level of theory with carbon located in the B1 and B2 positions of the octahedra as well as in the B3 position in the B_2 units (see Figure 1). The structure with carbon in the latter position is largely more stable than the other two structures with carbon located in B1 and B2 positions by 1.00 and 0.85 eV per $Ca_4B_{15}C$ formula, respectively. B3−C and B3−B3 distances of 1.626 and 1.682 Å are computed for this structure, and its cell parameters fit well with those determined experimentally. This leads to an averaged distance of 1.668 Å, close to the "B3−B3" distance measured experimentally by Meyer for $CaB_{3.75}C_{0.25}$ (1.670 Å)[13] and substantially shorter than the B3−B3 distance of 1.729 Å computed for CaB_4.

Conclusion

DFT calculations show that compounds with the ThB_4-type structure (including CaB_4) exhibit a pseudo gap for a count of 60 valence electrons per $M_4(B_6)_2(B_2)_2$ formula unit. This count satisfies the stability electron requirement for B_6^{2-} (20 electrons) and B_2^{2-} (8 electrons, see Scheme 1) units and allows the filling of two supplementary low-lying bands deriving from the valence metallic d atomic orbitals. This favored electron count is not reached for CaB_4 which is deficient by one electron per metal atom. This is likely the reason why only carbon-doped CaB_4 materials have been characterized so far. This raises the question of the existence of undoped CaB_4, whereas CaB_3C would possess the "ideal" electron count encountered in trivalent rare-earth metal tetraborides.

Acknowledgment. The authors thank the Institut de Développement et de Ressources en Informatique Scientifique (IDRIS-CNRS) and the Centre Informatique National de l'Enseignement Supérieur (CINES) for computing facilities. J.Y.S. thanks the Institut Universitaire de France (IUF) for support.

IC701967N